



due to a magnetic impurity in the  $J \rightarrow 0$  limit in the flat-band approximation.

## II. MODEL

We consider the Kondo impurity model

$$H = Js \cdot \mathbf{S} + \sum_{\mathbf{k}a} \epsilon_{\mathbf{k}} c_{\mathbf{k}a}^\dagger c_{\mathbf{k}a}, \quad (4)$$

where  $J$  is the Kondo exchange coupling constant,

$$\mathbf{s} = \frac{1}{2} \sum_{ab} f_a^\dagger \boldsymbol{\sigma}_{ab} f_b \quad (5)$$

is the local spin-density at the position of the impurity, with  $a, b \in \{\uparrow, \downarrow\}$  and the local operator at the origin  $f$  defined as

$$f_a^\dagger = \frac{1}{\sqrt{N}} \sum_{\mathbf{k}} c_{\mathbf{k}a}^\dagger, \quad (6)$$

$N$  being the number of sites forming the lattice,  $\mathbf{S}$  is the impurity spin-1/2 operator,

$$\mathbf{S} = \frac{1}{2} \boldsymbol{\sigma}, \quad (7)$$

and the conduction-band part of the Hamiltonian corresponds to either a 1D chain, a 2D square-lattice, or a 3D cubic-lattice tight-binding model. The only information about the conduction band that is relevant for the impurity model is its density of states  $\rho(\epsilon)$ , which is known in analytical form for all three dimensions. The chemical potential is measured from the bottom of the band, thus  $\mu = 0$  corresponds to a completely depleted band.

The calculations are done within the grand-canonical ensemble in the true thermodynamic limit, thus both the system size and the total number of electrons are infinite: the band filling  $n$  is controlled by  $\mu$ , while  $L, N \rightarrow \infty$ . The NRG discretization is performed using the method described in Ref. 6 which correctly handles arbitrary DOS even in the presence of singularities<sup>8</sup>. This approach allows to calculate the energy gain  $\Delta E$  to extremely high accuracy<sup>9</sup> by performing two NRG runs, one for a finite  $J$  and another for a reference system with decoupled impurity ( $J = 0$ ), then subtracting the obtained ground-state energies of the discrete Wilson-chain representations; while these two energies depend significantly on the details of the NRG discretization, their difference does not and, in fact, changes very little with varying value of the discretization parameter  $\Lambda$  if the appropriate discretization scheme is used<sup>9</sup>. The numerical calculations are performed for  $N_z = 8$  twisted discretization grids and with the discretization parameter  $\Lambda = 2^{3,6}$ . The truncation cutoffs are taken high enough so that the results are fully converged. The temperature is effectively zero. The results will be presented in units of half-bandwidth  $D = 2dt$ , where  $d$  is dimensionality of the tight-binding lattice.

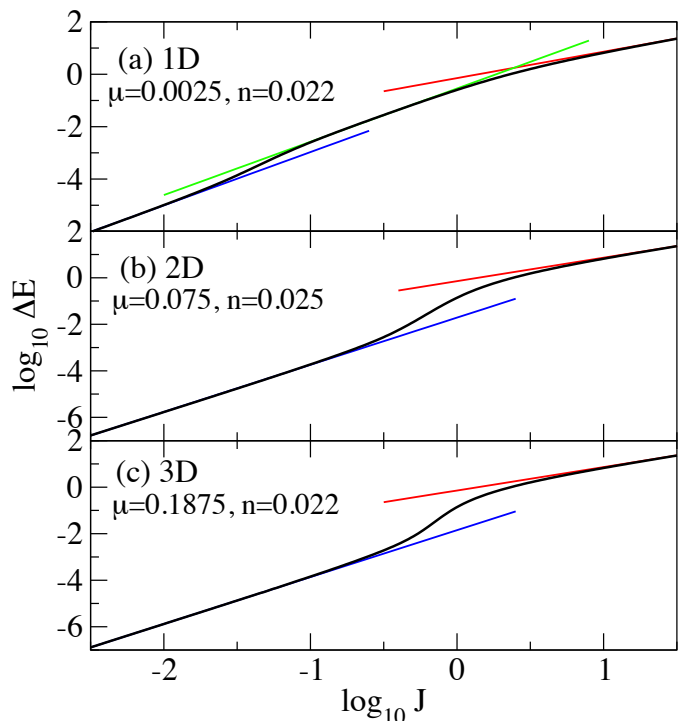


Figure 1. Overview of the different parameter regimes in the 1D, 2D, and 3D cases. The energy gain  $\Delta E$  is plotted as a function of the Kondo exchange coupling  $J$  on a log-log scale. The red and blue lines are the high- $J$  and low- $J$  asymptotics,  $\propto J$  and  $\propto J^2$ , respectively, common for all three dimensions. For 1D case in panel (a) we also indicate the intermediate- $J$  regime which is  $\propto J^2$  (green line). The model parameters are indicated in the respective panels. They are chosen so that the band occupancy is comparable in all three cases,  $n \approx 0.02$ .

## III. CHARACTERISTIC ENERGY SCALES

### A. Binding energy $\Delta E$

We first discuss the relevant parameter regimes of the exchange coupling  $J$ . We find that in all cases, irrespective of the energy-dependence of the DOS and the nature of the singularities, the small- $J$  and large- $J$  regimes behave exactly the same, see Fig. 1.

In the large- $J$  regime, we find the expected result that the energy gain is  $\Delta E = 3J/4$  due to the formation of a local singlet state between the impurity spin and the lattice site to which the impurity is attached. This regime is reached for  $J \gg D$ . In all cases considered, the numerical value of  $\Delta E$  lies atop the  $3J/4$  line within the accuracy of linewidth for  $J/D \gtrsim 10$ .

In the small- $J$  regime we find quadratic behavior with a non-universal prefactor  $\alpha$  that depends on the DOS ( $d = 1, 2, 3$ ) and the band occupancy  $n$ ,

$$\Delta E = \alpha_d(n) J^2. \quad (8)$$

It should be emphasized that  $\Delta E$  is not of the order of  $T_K$  for small  $J$ , as often claimed. The difference is perhaps under-

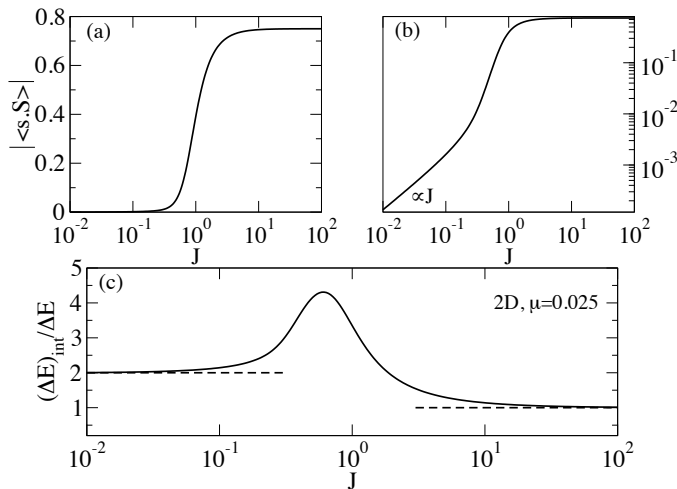


Figure 2. (a,b) Absolute value of the spin-spin expectation value,  $|\langle \mathbf{s} \cdot \mathbf{S} \rangle|$ , i.e., the correlation between the impurity spin and the conduction band spin at the location of the impurity, plotted on log-linear and log-log scales. (c) Ratio between the local contribution to the energy gain  $(\Delta E)_{\text{int}} = J|\langle \mathbf{s} \cdot \mathbf{S} \rangle| \propto J^2$ , and the total energy gain  $\Delta E$ . The calculations are performed for 2D DOS with  $\mu = 0.025$ .

appreciated, because the common intuition is that the energy gain in the formation of the Kondo singlet state should be approximately  $T_K$  since the singlet forms on that energy scale. In fact, the situation is somewhat more subtle because of the logarithmic scaling of the exchange coupling in the Kondo mechanism<sup>2,10</sup>. Many decades of bulk excitations above  $T_K$  (in the scaling regime  $T_K \ll \epsilon \ll J$ ) are already slightly perturbed by the exchange scattering off the magnetic impurity. The degree of perturbation can be quantified through the quasiparticle phase-shift of the bath electron with energy  $\epsilon$ ,  $\delta(\epsilon)$ . The phase shift for  $\epsilon \gg J$  is essentially zero, because in this range the bath electron spin is hardly affected by the impurity. The local moment starts to be felt on the energy scale  $\epsilon \sim J$ , but the effect is weak and the phase shift is  $\sim J/D$ . At still lower energies, the phase shift then increases logarithmically, until for  $\epsilon$  on the scale of  $T_K$  it reaches saturated values of the order of 1 (recall that  $\delta(\epsilon = 0) = \pi/2$  for the Kondo effect at the particle-hole symmetric point). The total energy gain is given as an integral of the single-particle energy shifts approximately proportional to  $\delta(\epsilon)$ , over all energies  $\epsilon$ , and since the contribution is  $\sim J$  for all  $\epsilon \lesssim J$ , we expect the result to scale as  $\Delta E \propto J^2$ . The behavior  $\Delta E \propto J^2$  is indeed seen in the numerical calculations of this quantity using the NRG in all models of this class. Since the Kondo problem is known to be non-perturbative in  $J$ , the actual expression must in fact be of the form  $\Delta E = f(J) + g(J)$ , where  $f(J)$  is an analytical function which is quadratic in the  $J \rightarrow 0$  limit, while  $g(J)$  is a non-analytical exponentially-small correction which may be neglected in the  $J \rightarrow 0$  limit compared to the first term. The leading correction due to dynamical processes in  $f(J)$  is actually  $O(J^3)$ , hence analytical, see Appendix B.

Another quantity of interest is the expectation value of  $\langle \mathbf{S} \cdot \mathbf{s} \rangle$ , i.e., of the interaction term in the Kondo Hamiltonian. Since this term is coupled linearly to  $J$ , it can be esti-

mated through  $d\langle H \rangle/dJ = -d\Delta E/dJ$ . Since  $\langle \mathbf{S} \cdot \mathbf{s} \rangle \propto J$ , see Fig. 2(a,b), by integration of  $\Delta E$  over  $J$  we again find  $\Delta E \propto J^2$ . In fact, it is interesting to compare  $\Delta E$  with the quantity

$$(\Delta E)_{\text{int}} = J|\langle \mathbf{S} \cdot \mathbf{s} \rangle|, \quad (9)$$

see Fig. 2(c). As expected, in the large- $J$  limit the full contribution to the energy gain comes from the singlet localized at the position of the impurity. The low- $J$  limit of the ratio  $(\Delta E)_{\text{int}}/\Delta E$  is exactly 2; this is found universally for all values of filling and for all three dimensionalities. In fact, this follows directly from the quadratic behavior of  $\Delta E$ . Namely,

$$\frac{(\Delta E)_{\text{int}}}{\Delta E} = \frac{J(d\Delta E/dJ)}{\Delta E} = \frac{d \ln \Delta E}{d \ln J}, \quad (10)$$

thus the plot in Fig. 2(c) actually represents the logarithmic derivative of  $\Delta E$  from which we can directly read off the local power-law exponent  $\beta$  at given  $J$ . It then follows that

$$\begin{aligned} (\Delta E)_{\text{int}} &= \beta \Delta E, \\ (\Delta E)_{\text{kin}} &= (1 - \beta) \Delta E, \end{aligned} \quad (11)$$

where the kinetic part  $(\Delta E)_{\text{kin}} = (\Delta E) - (\Delta E)_{\text{int}}$ . This result indicates that asymptotically, for  $J \rightarrow 0$ , twice the binding energy is always contributed by the local  $\mathbf{s}(\mathbf{r} = 0)$  term, while the kinetic part  $(\Delta E)_{\text{kin}}$  is actually negative and equal in absolute value to  $\Delta E$ . In the high- $J$  limit, we have  $\beta = 1$ , thus the energy gain is entirely due to the local interaction term with no correction from the bulk. Fig. 2(c) also indicates that  $\beta > 1$  at any finite  $J$ , thus the binding (energy gain) is always due to the interaction term, while the kinetic term always reduces the binding since it is strictly negative.

Returning now to the discussion of the different regimes of  $J$  in relation to Fig. 1, we note a clear difference between the 2D and 3D compared to the 1D case. In 2D and 3D, the low- $J$  and high- $J$  asymptotic regimes of  $\Delta E$  are connected by a single sigmoidal cross-over curve whose inflection point is slightly below  $J = 1$ , and the low- $J$  asymptotic regime is reached at  $J \approx 0.2$ . In 1D, the behavior is qualitatively different: at  $J \approx 3$  we observe a very smooth crossover from the  $3J/4$  behavior to an intermediate  $J^2$  regime which extends to very low  $J$  values, then at  $J \approx 0.03$  there is a crossover to the asymptotic weak-coupling  $J^2$  regime with a different prefactor, see Fig. 1(a). This is, in fact, the physics discussed in Ref. 1: when the characteristic energy scale, such as  $\Delta E$  or  $T_K$ , is larger than  $\mu$ , the system is sensitive to the diverging DOS at the bottom of the conduction band in one dimension and the system is in a different universality class, namely the class associated with the density of states that diverges as a power-law at the Fermi level<sup>11</sup>. When the characteristic scale is below  $\mu$ , however, we recover the more conventional Kondo screening behavior as found in 2D and 3D.

## B. Kondo temperature $T_K$

We now directly compare the energy gain  $\Delta E$  and the Kondo temperature  $T_K$  in Fig. 3. We recall that  $T_K$  is de-

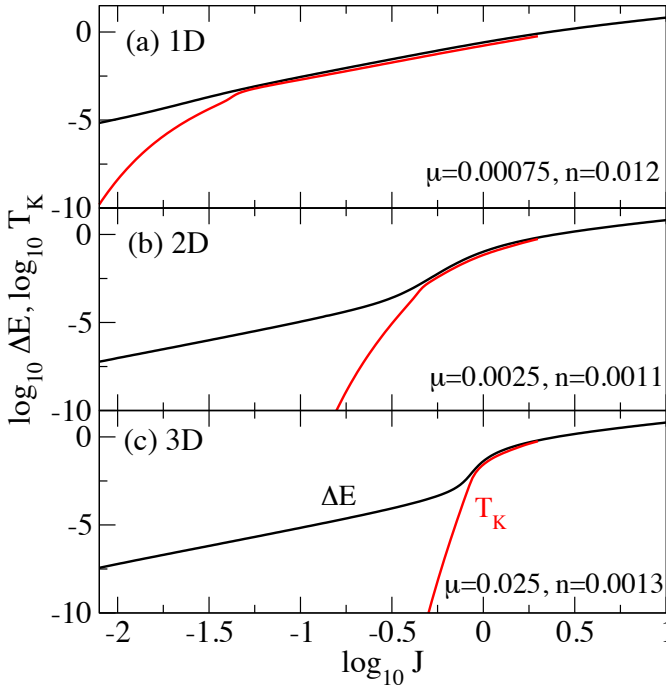


Figure 3. Relation between the energy gain  $\Delta E$  and the Kondo temperature  $T_K$  for three different dimensionalities. The two quantities behave similarly only in the intermediate-coupling regime, but have very different weak-coupling asymptotic behavior.

financed thermodynamically through the impurity magnetic susceptibility according to Wilson's prescription  $T_K \chi_{\text{imp}}(T_K) = 0.07^3$ . This is thus the temperature scale on which the impurity magnetic moment becomes quenched, irrespective of the mechanism how this actually occurs (via Kondo effect of conventional or unconventional type, or via local singlet formation). We find that the two quantities are proportional in the cross-over intermediate- $J$  and large- $J$  regimes,  $\Delta E \approx c T_K$ , where  $c$  is a non-universal prefactor of the order of 1. For large  $J$ ,  $T_K$  cannot be directly calculated in the NRG, but our definition through moment quenching is consistent with  $T_K$  behaving as  $T_K \sim J$  in the large- $J$  limit, thus in this sense the proportionality persists there. For small  $J$ , however,  $T_K$  behaves exponentially,

$$T_K \sim \exp(-1/\rho_0 J), \quad (12)$$

while  $\Delta E$  is quadratic, as discussed above. (Here  $\rho_0 = \rho(\mu)$  is the density of states at the Fermi level, which depends on the value of electron density  $n$ .) Indeed, we find that the lower- $J$  boundary of the intermediate- $J$  regime is defined precisely by the point where the two quantities run apart. This is especially pronounced in 1D<sup>1</sup>, but also occurs in 2D and 3D.

### C. Onset of the Kondo scaling regime

The difference between  $\Delta E$  and  $T_K$  in the weak-coupling limit for  $T_K < \mu$  should not be too surprising, because the

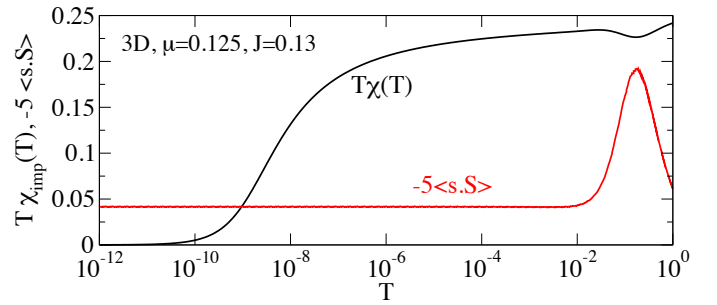


Figure 4. Temperature dependence of the impurity magnetic susceptibility  $T\chi_{\text{imp}}(T)$  and of the spin-spin correlation  $\langle \mathbf{s} \cdot \mathbf{S} \rangle$ , in the parameter regime where  $\Delta E$  and  $T_K$  are already significantly separated.

Kondo effect is something which happens in the conduction band due to the presence of the impurity, possibly involving bulk electrons far away from its position, while the impurity binding is more locally sensitive. It is also interesting to compare the temperature dependences of the impurity susceptibility  $T\chi_{\text{imp}}(T)$  and of the expectation value  $\langle \mathbf{s} \cdot \mathbf{S} \rangle(T)$ , see Fig. 4. It is found that the expectation value reaches its saturated value on the scale  $T \sim 10^{-2}$ , significantly above  $\Delta E$  which is here equal to  $4 \times 10^{-4}$ , while the impurity local moment is quenched at much lower temperatures.

If, however, a similar comparison is performed in the parameter range where  $\Delta E$  and  $T_K$  are proportional, i.e., for  $T_K > \mu$ , we find that both  $T\chi_{\text{imp}}(T)$  and  $\langle \mathbf{s} \cdot \mathbf{S} \rangle(T)$  saturate on the same temperature scale. In addition, we find that  $T\chi_{\text{imp}}(T)$  does not show universal Kondo behavior at low temperatures in such cases.

From these observations we conclude that the separation between  $\Delta E$  and  $T_K$  is actually a sign of the onset of a true conventional Kondo effect where the spin is quenched through the gradual scaling of the effective exchange coupling  $J$  from a small bare value  $J$  to the strong coupling regime, so that the thermodynamic quantities show universal behavior. This regime occurs when the Kondo temperature is smaller than the distance of the Fermi level from the band edge, as quantified by  $\mu$ .

All other cases, where  $\Delta E \propto T_K$ , are an indication of unconventional local moment quenching mechanisms, either through the trivial local singlet formation for large- $J$ , or through an unconventional flow of the RG equations due to extreme particle-hole asymmetry due to diverging DOS, as in the 1D case. To conclude: as soon as the physics is appreciably and simultaneously affected by the band on all energy scales, including the states at the very edge of the band, so that the energy scales can no longer be nicely separated into logarithmic chunks, the binding energy  $\Delta E$  and the local moment quenching scale  $T_K$  become equivalent.

## IV. KONDO TEMPERATURE AT LOW DENSITY

### A. Prefactors

Finally, we discuss the quantitative effects of the band-edge singularities in the DOS on the scaling of the Kondo temperature against  $J$ . We plot the logarithm of the Kondo temperature versus  $1/\rho_0 J$ , where  $\rho_0$  is the density of states at the Fermi level, for a range of  $n$  from the half-filling,  $n = 1/2$ , to very small values of the density, see Fig. 5. The non-universal behavior for intermediate and large  $J$  is due to band-edge singularities and therefore depends on the dimensionality of the system. For small  $J$ , however, the exponential behavior  $T_K \sim \exp(-1/\rho_0 J)$  is always eventually recovered and we find straight lines with essentially equal slope. We emphasize that the main effect of the  $n$ -dependence is already included through the DOS at the Fermi level,  $\rho_0 = \rho(\mu)$ , thus the trend indicated by the arrows in the figure (oriented from half-filling to small  $n$  range) is due to the differences contained in the prefactor  $c_d(\mu)$  to the exponential term in the expression for  $T_K$ :

$$T_K = c_d(\mu) \exp[-1/\rho_0 J].$$

Here we find notable differences that can be ascribed solely to the dimensionality-dependent singularities in the DOS: in 1D, the prefactor  $c_1$  at constant  $\rho_0 J$  decreases with decreasing filling  $n$ , leading to lower  $T_K$ , while exactly the opposite behavior is found in the prefactor  $c_3$  for the 3D case; the 2D case is in the intermediate situation with curves that are overlapping to a good approximation, hence  $c_2$  is approximately constant. To be more precise, close to the band-edge (for  $\mu$  small compared to the half-bandwidth  $D = 2dt$ ), we find that the prefactors  $c_d(\mu)$  can be approximated fairly well as

$$\begin{aligned} c_1 &\approx \mu, \\ c_2 &\approx D, \\ c_3 &\approx 25.5D \exp[-9.5\sqrt{\mu/D}]. \end{aligned} \quad (13)$$

### B. Scaling equations for particle-hole asymmetric band

The differences between the three dimensionalities are too large to be ascribed solely to the effect of the filling-dependence of the effective bandwidth. Instead, they must be ascribed to the renormalization of the exchange coupling due to potential scattering,  $\rho_0 J \rightarrow \rho_0 J_{\text{eff}}$ . There is no bare potential term in the Hamiltonian, but it is generated by the renormalization flow when the particle-hole symmetry is broken away from half-filling. We now provide an analytical account of this behavior. The scaling equations for the spin-1/2 Kondo model with the Hamiltonian expressed in the form

$$H_{\text{imp}} = \mathbf{J}\mathbf{S} \cdot \mathbf{s} + Vn, \quad (14)$$

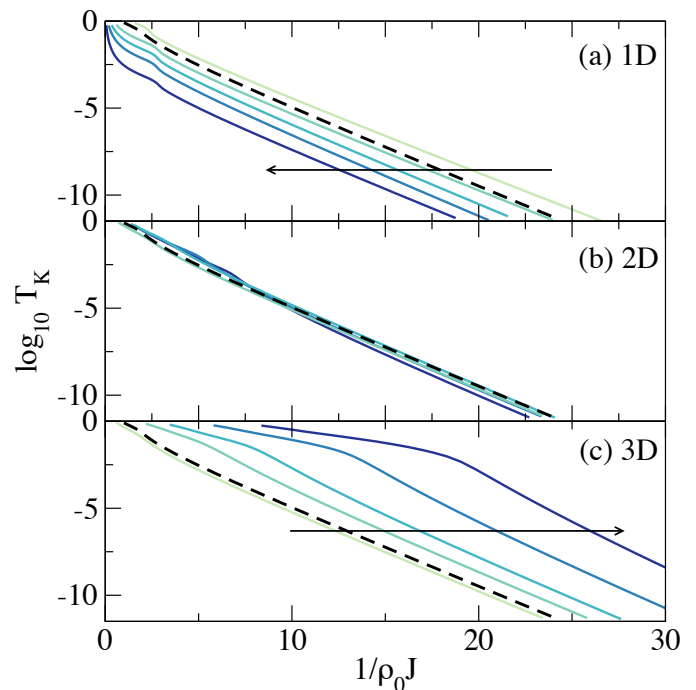


Figure 5. Asymptotic scaling of the Kondo temperature. We plot the logarithm of  $T_K$  versus  $1/\rho_0 J$ , where  $\rho_0$  is the density of states in the conduction band at the Fermi level,  $\rho_0 = \rho(\mu)$ . The dashed line indicates the standard result for a flat density of states. The arrows indicate the direction of reduced band filling  $n$ , i.e., going toward a more asymmetric situation. In (a) we plot  $n = 0.012, 0.041, 0.074, 0.12$ , and  $0.5$ , in (b) we plot  $n = 0.0011, 0.0083, 0.085$ , and  $0.39$ , (c) we plot  $n = 0.0013, 0.0032, 0.012, 0.035$ , and  $0.5$ .

where  $V$  is the potential and  $n = \sum_a f_a^\dagger f_a$  is the local density of bulk electrons at the position of the impurity, are<sup>2,12</sup>

$$\begin{aligned} \frac{dJ}{d \ln D} &= -\frac{\rho_+}{2} J^2 + 2\rho_- J V, \\ \frac{dV}{d \ln D} &= \rho_- \left( \frac{3}{16} J^2 + V^2 \right), \end{aligned} \quad (15)$$

where

$$\begin{aligned} \rho_+ &= \rho(D) + \rho(-D), \\ \rho_- &= \rho(D) - \rho(-D), \end{aligned} \quad (16)$$

are the symmetric and antisymmetric combination of the density of states in the empty and filled parts of the band, with the energy argument  $\epsilon$  of  $\rho(\epsilon)$  now measured with respect to the Fermi level. These equations are fully general and are valid for arbitrary  $\rho(\epsilon)$ .

It has been shown that the potential scattering in asymmetric bands with non-zero  $\rho_-$  may play an important role<sup>12</sup>. By inspection of the scaling equation for  $J$  we see that if  $V$  and  $\rho_-$  are of the same sign, the growth of  $J$  with decreasing bandwidth slows down ( $T_K$  is reduced), and the opposite is the case if  $V$  and  $\rho_-$  are of opposite signs ( $T_K$  is increased). The scaling equation for  $V$  tells that if the bare  $V$  is zero, effective potential scattering will be generated by the exchange scattering in second order so that  $V$  is of the *opposite* sign as  $\rho_-$ .

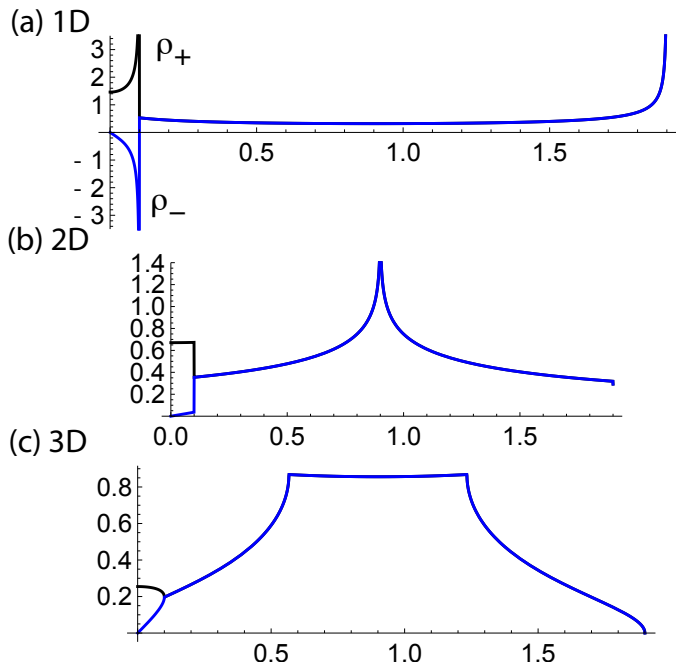


Figure 6. Symmetric and antisymmetric combination of the conduction-band density of states that affects the renormalization flow:  $\rho_{\pm}(\epsilon) = \rho(\epsilon) \pm \rho(-\epsilon)$ . Here  $\mu = 0.1$ .

Thus, an asymmetric DOS might be expected to always lead to a higher Kondo temperature irrespective of the sign of  $\rho_-$ .

We now consider our actual problem to see that the situation is slightly more subtle. There are two energy regions. In the high-energy region (i) for  $|\epsilon| > \mu$  only the renormalization due to the non-occupied high-energy states between  $\mu$  and the upper band edge  $D$  contributes. Then  $\rho_+(\epsilon) = \rho_-(\epsilon) = \rho(+\epsilon) > 0$ , see Fig. 6. This will generate a potential scattering  $V$  with a negative sign. While the detailed form of  $\rho$  depends on the dimensionality, the qualitative behavior is the same in all three cases.

In the low-energy region (ii) for  $|\epsilon| < \mu$  there will be both particle-like and hole-like processes. The behavior of  $\rho_+$  and  $\rho_-$  in this region strongly depends on the dimensionality, because close to the band edge  $\rho$  is concave in 3D, approximately flat in 2D, and convex in 1D. For this reason, in 3D  $\rho_-$  is positive, in 2D  $\rho_-$  is approximately zero, while in 1D  $\rho_-$  is negative, see Fig. 6, and these differences become increasingly pronounced the closer  $\mu$  gets to the band edge due to the curvature of the DOS. Thus, in 3D  $V\rho_- < 0$  and  $T_K$  will tend to be increased, as indeed observed in Fig. 5(c) for increasingly asymmetric band (smaller electron density), as indicated by the arrow. In 1D, however,  $V\rho_- > 0$  and  $T_K$  will be reduced, again in line with the NRG results in Fig. 5(a). Finally, in 2D with  $\rho_- \approx 0$  due to the approximate flatness, the potential scattering term does not play a significant role in the renormalization of  $J$ , thus we recover results which nearly overlap with those obtained in the flat-band approximation, see Fig. 5(b).

The numerical solutions of the scaling equations can indeed

be fitted to  $T_K = c_d(\mu) \exp(-1/\rho_0 J)$  with  $c_d(\mu)$  given by Eqs. (13) with some small deviations due to the scaling equations being truncated at the second order in  $J$  and  $V$ , while the NRG includes processes to all orders.

## V. CONCLUSION

This work explored two issues: 1) the characteristic low-energy scales of the Kondo impurity model, focusing in particular on the difference between the binding energy  $\Delta E$  and the local-moment quenching scale  $T_K$ , 2) the effects due to the band-edge van Hove singularities characteristic of the different dimensionalities of the conduction band, which lead to significant effects in the regime of very low electron density. We showed that in the asymptotic weak-coupling low- $J$  (scaling) regime the binding energy is quadratic in  $J$ , while the Kondo temperature is exponentially small. While it is meaningful to compare the scale  $T_K$  to other magnetic coupling scales (such as the RKKY coupling  $J_{\text{RKKY}}$ ) when discussing the competition between the Kondo screening and magnetic ordering, because this decides the fate of the effective moment for temperatures below  $\max(T_K, J_{\text{RKKY}})$ , this does not imply that an isolated impurity reduces the total ground state energy only by  $T_K$ . Instead,  $T_K$  is only a minor correction to the total energy gain arising from the exchange coupling of the impurity with bulk electrons, which is  $\propto J^2$ . As concerns the dimensionality, we find that the case of 2D is the closest to the conventional Kondo scenario, because in the relevant low-energy range the 2D DOS is approximately flat. For low  $J$ , the Kondo temperature is thus given by the standard expression  $T_K \approx D \exp(-1/\rho_0 J)$ . In 1D and 3D we find notable deviation in opposing directions. For the 3D case with concave DOS, the Kondo temperature is increased for reduced band filling:  $T_K \approx 25.5D \exp[-9.5\sqrt{\mu/D}] \exp(-1/\rho_0 J)$ . For the 1D case, we find that the Kondo temperature in some range of exchange couplings  $J$  such that  $T_K > \mu$  is a quadratic function of  $J$ , while for small  $J$  the exponential dependence is recovered. Since the 1D DOS is convex, we find that the Kondo temperature decreases compared to the standard flat-band value for reduced band filling:  $T_K \approx \mu \exp(-1/\rho_0 J)$ .

Similar trends are expected for other impurity models such as the Anderson impurity model. There the detailed behavior will also depend on the intrinsic potential scattering (bare  $V$  after the Schrieffer-Wolff transformation). It should also be noted that in the context of the dynamical mean-field theory (DMFT) the effective impurity model is actually in the intermediate coupling regime where  $\Delta E \propto T_K$ , thus the energy gain and the coherence temperature are expected to be of the same scale.

## ACKNOWLEDGMENTS

The authors acknowledge the support of the Slovenian Research Agency (ARRS) under P1-0044 and J1-7259, and thank Jernej Mravlje for comments.

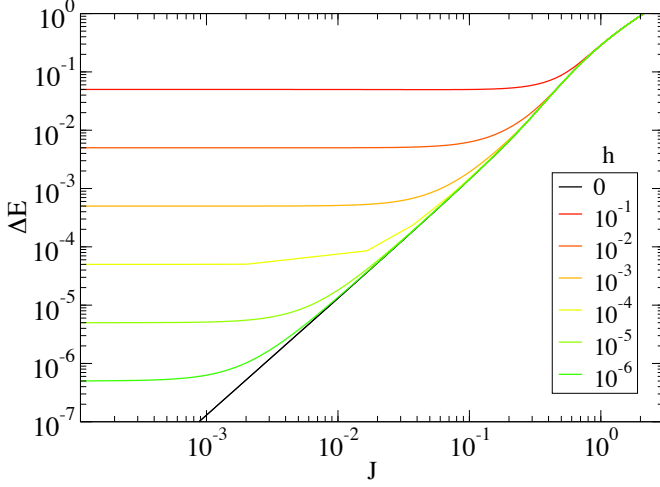


Figure 7. Energy gain  $\Delta E$  in the presence of the magnetic field. Here we use a flat band and the chemical potential is fixed in the center of the band.

### Appendix A: Magnetic field effects

We now briefly consider the energy gain of the impurity in the presence of the Zeeman term in the Hamiltonian:

$$H_{\text{Zeeman}} = g_{\text{imp}} \mu_B B S_z + \sum_k g_{\text{bulk}} \mu_B B s_{z,k}. \quad (\text{A1})$$

We take  $g \equiv g_{\text{imp}} = g_{\text{bulk}}$ , and express the field in units of the Zeeman energy,  $h = g \mu_B B$ . The results, displayed in Fig. 7, show the expected result: for small  $J$  the energy gain saturates at the value  $\Delta E = h/2$  with the cross-over occurring for  $J$  such that  $\Delta E \approx h/2$ . The value of  $T_K$  does not play any role here.

### Appendix B: Anisotropic Kondo coupling

The XXZ anisotropic Kondo model takes the following form:

$$H_{\text{XXZ}} = J_{\parallel} S_z s_z + J_{\perp} (S_x s_x + S_y s_y). \quad (\text{B1})$$

The extreme case is that of Ising-like coupling,  $J_{\perp} \equiv 0$ . There is no impurity dynamics in this limit and the Hamiltonian becomes quadratic, hence exactly diagonalisable (see the following Appendix). In the small- $J$  and high- $J$  limits, the energy gain for Ising coupling with  $J_{\parallel} = J$  is one third of that in the regular isotropic Kondo model with Heisenberg coupling  $J_{\parallel} = J_{\perp} = J$ , while the non-trivial deviations due to many-particle physics occur in the intermediate- $J$  range, see Fig. 8. The energy gain is always larger in the isotropic model even after accounting for the overall factor of 3. In the small- $J$  asymptotic regime where  $\Delta E_{\text{Heisenberg}} \approx 3 \times \Delta E_{\text{Ising}}$  to a good approximation, the Kondo temperature is smaller than  $\Delta E$  already by many orders of the magnitude.

We have also computed the difference of the energy gain for isotropic exchange and three times the energy gain for Ising

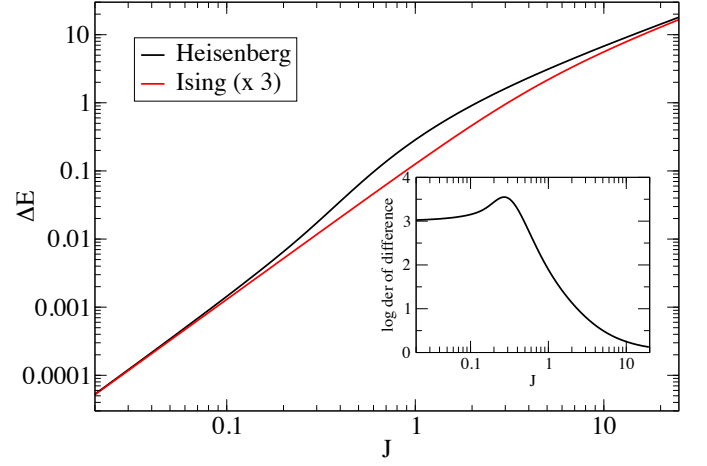


Figure 8. Energy gain  $\Delta E$  in anisotropic Kondo model with exchange coupling of Ising type,  $J_{\parallel} = J$  and  $J_{\perp} = 0$ , and in the isotropic model with exchange coupling of Heisenberg type,  $J_{\parallel} = J_{\perp} = J$ . The result for the Ising coupling is multiplied by 3 for easier comparison. We use a flat band with  $\mu$  fixed in its center. The inset shows the logarithmic derivative of  $(\Delta E)_{\text{Heisenberg}} - 3(\Delta E)_{\text{Ising}}$ , thus indicating the power-law exponent of the correction due to spin-flip dynamics.

coupling. The result is plotted as the inset in Fig. 8 in the form of the logarithmic derivative of the quantity. Considering that the quadratic term in the energy gain is entirely due to the spin-dependent scattering on a static local moment, we see that the leading contribution to the ground state energy of the spin-flip processes leading to the Kondo effect is of the order of  $J^3$  (and not  $T_K$ ).

### Appendix C: Energy gain in the $J \rightarrow 0$ limit

The energy gain in the small- $J$  limit will now be calculated analytically. The calculation is performed using the equations of motion for a static impurity in the bulk:

$$H_{\text{kin}} = \sum_{k\sigma} \epsilon_k c_{k\sigma}^{\dagger} c_{k\sigma}, \quad (\text{C1})$$

$$H_{\text{int}} = (2h) s_z(\mathbf{r} = 0),$$

The factor 2 in  $(2h)$  is included for convenience. For  $S = 1/2$  impurity,  $h = J/4$ . We now drop the spin index  $\sigma$  and focus on the  $\sigma = \uparrow$  case; the sums over spin are performed by taking  $h \rightarrow -h$  for  $\sigma = \downarrow$ . The energy gain is defined as

$$\Delta E = \langle H \rangle_{J=0} - \langle H \rangle_J, \quad (\text{C2})$$

and can be split into two contributions:

$$\Delta E = (\Delta E)_{\text{kin}} + (\Delta E)_{\text{int}}. \quad (\text{C3})$$

For the impurity  $T$ -matrix we find

$$T(z) = \frac{1}{N} [h + h^2 \langle \langle f; f^{\dagger} \rangle \rangle_z], \quad (\text{C4})$$

where  $N$  is the number of lattice sites in the system, and  $f = (1/\sqrt{N}) \sum_k c_k$ , so that the  $k$ -resolved Green's function is

$$G_{kk'}(z) = G_k^0(z)\delta_{kk'} + G_k^0(z) \frac{1}{N} [h + h^2 \langle \langle f; f^\dagger \rangle \rangle_z] G_{k'}^0(z), \quad (\text{C5})$$

with  $G_k^0(z) = (z - \epsilon_k)^{-1}$  being the non-perturbed bulk Green's function. We note that

$$G_f(z) \equiv \langle \langle f; f^\dagger \rangle \rangle_z = \frac{1}{N} \sum_{kk'} G_{kk'}(z), \quad (\text{C6})$$

hence we sum over  $k$  and  $k'$  to obtain

$$G_f(z) = G_{\text{loc}}^0(z) + G_{\text{loc}}^0(z) [h + h^2 G_f(z)] G_{\text{loc}}^0(z). \quad (\text{C7})$$

The solution is

$$G_f(z) = \frac{G_{\text{loc}}^0(z)}{1 - h G_{\text{loc}}^0(z)}. \quad (\text{C8})$$

For a flat band with half-bandwidth  $D$ , the exact expression for  $G_{\text{loc}}^0(z)$  is

$$G_{\text{loc}}^0(z) = -\frac{1}{2D} \ln \frac{z - D}{z + D}. \quad (\text{C9})$$

We now calculate the energy gain due to the interaction term,  $(\Delta E)_{\text{int}} = -\langle H_{\text{int}} \rangle = -h(n_{f\uparrow} - n_{f\downarrow})$ , with

$$n_{f\sigma} = \langle f_\sigma^\dagger f_\sigma \rangle = \int_{-\infty}^{\infty} f(\omega) d\omega \frac{-1}{\pi} \text{Im} G_{f\sigma}(z), \quad (\text{C10})$$

$f(\omega)$  being the Fermi function. We take the difference

$$h [G_{f\uparrow}(z) + (h \rightarrow -h)] = \frac{2h^2 G_{\text{loc}}^0(z)}{1 - h^2 [G_{\text{loc}}^0(z)]^2} \approx 2h^2 [G_{\text{loc}}^0(z)]^2. \quad (\text{C11})$$

Then

$$(\Delta E)_{\text{int}} = \frac{2h^2}{\pi} \int_{-\infty}^{\infty} \text{Im} \left\{ [G_{\text{loc}}^0(\omega + i\delta)]^2 \right\} f(\omega) d\omega. \quad (\text{C12})$$

---

The first term in  $G_{kk}$  cancels out after subtracting the energy of the system without the impurity. Thus

$$(\Delta E)_{\text{kin},\sigma} = \frac{1}{\pi} \sum_k \epsilon_k \int_{-\infty}^{\infty} d\omega \text{Im} \left( \frac{1}{z - \epsilon_k} \frac{1}{N} [h + h^2 G_f(z)] \frac{1}{z - \epsilon_k} \right) f(\omega). \quad (\text{C19})$$

This has to be summed over spin. Recalling that  $h$  changes sign, the first term cancels out and

$$h^2 [G_f(z) + (h \rightarrow -h)] = 2h^2 \frac{G_{\text{loc}}^0(z)}{1 - h^2 [G_{\text{loc}}^0(z)]^2} \approx 2h^2 G_{\text{loc}}^0(z). \quad (\text{C20})$$

For small  $h$  we are left with ( $z = \omega + i\delta$ )

$$\begin{aligned} \Delta E_1 &= 2 \frac{h^2}{\pi} \frac{1}{N} \sum_k \epsilon_k \int_{-\infty}^{\infty} d\omega \text{Im} \left( \frac{1}{z - \epsilon_k} G_{\text{loc}}^0(z) \frac{1}{z - \epsilon_k} \right) f(\omega) \\ &= 2 \frac{h^2}{\pi} \int \epsilon \rho(\epsilon) d\epsilon \int_{-\infty}^{\infty} d\omega \text{Im} \left( \frac{1}{z - \epsilon} G_{\text{loc}}^0(z) \frac{1}{z - \epsilon} \right) f(\omega). \end{aligned} \quad (\text{C21})$$

Noting that for  $z = \omega + i\delta$ ,

$$\text{Im}[G_{\text{loc}}^0(z)]^2 = 2 \text{Im} G_{\text{loc}}^0(z) \text{Re} G_{\text{loc}}^0(z) = 2\pi \rho^2 \ln \frac{D - \omega}{D + \omega}, \quad (\text{C13})$$

and integrating over  $\omega$  at  $T = 0$ , we finally find

$$(\Delta E)_{\text{int}} = 8 \ln 2 (\rho h)^2 = \frac{\ln 2}{8} (J/D)^2. \quad (\text{C14})$$

The total energy gain can now be computed using the formula

$$\Delta E = \int_0^J \frac{dJ'}{J'} \langle H_1 \rangle_{J'}, \quad (\text{C15})$$

where the expectation value is that of the interaction part of the Hamiltonian, here equal to  $(\Delta E)_{\text{int}}$  evaluated at  $J = J'$ , see also Eq. (11) with  $\beta = 2$ . Alternatively, we can explicitly calculate the band contribution  $(\Delta E)_{\text{bulk}}$ . The kinetic energy is

$$E_{\text{kin}} = \sum_k \epsilon_k n_k, \quad (\text{C16})$$

with

$$n_k = \int_{-\infty}^{\infty} A_k(\omega) f(\omega) d\omega, \quad (\text{C17})$$

and

$$A_k(\omega) = -\frac{1}{\pi} \text{Im} G_{kk}(\omega + i\delta). \quad (\text{C18})$$

The  $\epsilon$ -integral can be evaluated for a flat band (using  $D = 1$ ):

$$\int_{-1}^1 \frac{\epsilon}{(z - \epsilon)^2} d\epsilon = \frac{2z}{z^2 - 1} + \ln \frac{z - 1}{z + 1} \equiv F(z). \quad (\text{C22})$$

Then at  $T = 0$

$$(\Delta E)_{\text{kin}} = -\frac{2(h\rho)^2}{\pi} \text{Im} \left( \int_{-\infty}^0 F(\omega + i\delta) g(\omega + i\delta) d\omega \right), \quad (\text{C23})$$

where  $g(z) = -\ln \frac{z-D}{z+D}$ . The integration gives  $2\pi \ln 2$ . Thus

$$(\Delta E)_{\text{kin}} = -\frac{\ln 2}{16} (J/D)^2. \quad (\text{C24})$$

We finally obtain

$$\Delta E = \frac{\ln 2}{16} (J/D)^2. \quad (\text{C25})$$

This agrees within a few percent with the numerical renormalization group results for the gain in the ground state energy in the small- $J$  limit of an Ising-coupled magnetic impurity. For a full isotropic coupling, we find exactly three times as much:

$$\Delta E = \frac{3 \ln 2}{16} (J/D)^2, \quad (\text{C26})$$

again in full agreement with the numerical calculation. The leading correction due to dynamic processes is  $O(J^3)$ , as demonstrated in the previous Appendix.

- <sup>1</sup> Yulia E Shchadilova, Matthias Vojta, and Masudul Haque, “Single-impurity Kondo physics at extreme particle-hole asymmetry,” *Physical Review B* **89**, 104102 (2014).
- <sup>2</sup> A. C. Hewson, *The Kondo Problem to Heavy-Fermions* (Cambridge University Press, Cambridge, 1993).
- <sup>3</sup> K. G. Wilson, “The renormalization group: Critical phenomena and the Kondo problem,” *Rev. Mod. Phys.* **47**, 773 (1975).
- <sup>4</sup> H. R. Krishna-murthy, J. W. Wilkins, and K. G. Wilson, “Renormalization-group approach to the Anderson model of dilute magnetic alloys. I. Static properties for the symmetric case,” *Phys. Rev. B* **21**, 1003 (1980).
- <sup>5</sup> Ralf Bulla, Theo Costi, and Thomas Pruschke, “The numerical renormalization group method for quantum impurity systems,” *Rev. Mod. Phys.* **80**, 395 (2008).
- <sup>6</sup> Rok Žitko and Thomas Pruschke, “Energy resolution and discretization artefacts in the numerical renormalization group,” *Phys. Rev. B* **79**, 085106 (2009).
- <sup>7</sup> Rok Žitko, “Adaptive logarithmic discretization for numerical renormalization group methods,” *Comp. Phys. Comm.* **180**, 1271 (2009).
- <sup>8</sup> Rok Žitko, Janez Bonča, and Thomas Pruschke, “Van Hove singularities in the paramagnetic phase of the Hubbard model: a DMFT study,” *Phys. Rev. B* **80**, 245112 (2009).
- <sup>9</sup> Rok Žitko, “Numerical renormalization group calculations of ground-state energy: Application to correlation effects in the adsorption of magnetic impurities on metal surfaces,” *Phys. Rev. B* **79**, 233105 (2009).
- <sup>10</sup> J. Kondo, “Ground-state energy shift due to the  $s$ - $d$  interaction,” *Phys. Rev.* **154**, 644 (1967).
- <sup>11</sup> Andrew K Mitchell, Matthias Vojta, Ralf Bulla, and Lars Fritz, “Quantum phase transitions and thermodynamics of the power-law Kondo model,” *Physical Review B* **88**, 195119–12 (2013).
- <sup>12</sup> O Ujsaghy, K Vladar, G Zaránd, and A Zawadowski, “The Role of Electron-Hole Symmetry Breaking in the Kondo Problems,” *Journal of Low Temperature Physics* **126**, 1221–1231 (2002).